Thermodynamic Insights on the Feasibility of Homogeneous Batch Extractive Distillation. 2. Low-Relative-Volatility Binary Mixtures with Heavy Entrainer.

Ivonne Rodriguez-Donis, Vincent Gerbaud, Xavier Joulia

Thermodynamic Insights on the Feasibility of Homogeneous Batch Extractive Distillation. II. Low Relative Volatility Binary Mixtures with Heavy Entrainer.

Ivonne Rodriguez-Donis [1]

[1] *Instituto Superior de Tecnologías y Ciencias Aplicadas (INSTEC), Ave. Salvador Allende Luaces, Plaza, Ciudad de la Habana,, Cuba*

Vincent Gerbaud [2,3]* **and Xavier Joulia**[2,3]

[2]*Université de Toulouse, INP, UPS, LGC (Laboratoire de Génie Chimique), 5 rue Paulin Talabot, F-31106 Toulouse Cedex 01 – France*

[3]*CNRS, LGC (Laboratoire de Génie Chimique), F-31106 Toulouse Cedex 01 – France*

* corresponding author: Vincent.Gerbaud@ensiacet.fr

Abstract

All former studies reported that the separation of the low relative volatility binary mixture by using a heavy entrainer in a batch rectifier imposed the obligatory withdrawal of the most volatile original component. In this paper, we demonstrate that this does not always happen and that the product sequence can be unambiguously determined from the sole analysis of thermodynamic properties of residue curve maps and the occurrence of unidistribution lines and univolatility lines, following the general feasibility criterion enounced in part I for the separation of azeotropic mixtures using heavy or light entrainers. For low relative volatility mixtures, the original component having an intermediate boiling temperature can be also drawn as the first distillate product. Cases concerning 94% of statistically occuring zeotropic ternary mixtures are investigated, allowing to define the product sequence without any previous calculation of the liquid composition profile inside the column. Preliminary feasibility results are confirmed by computing maps of extractive and rectifying liquid composition profiles using a simplified mass balance. Final validation is done via rigourous simulation using ProSim Batch software.

1. Introduction

Despite its apparent simplicity, synthesis and design of batch distillation processes for separating a low volatility binary mixture (A) – (B) can be as difficult as for azeotropic mixtures. We assume that (A) is more volatil than (B). Usually, the binary liquid – vapour equilibrium is not sensitive enough to the pressure variation to undertake pressure swing distillation and either azeotropic or extractive distillation processes are required, both demanding the addition of an auxiliary component, so-called entrainer (E). Extractive distillation process where a homogeneous entrainer is fed to column side during the operation is our main concern, with no new azeotrope with the original components to split. Light or heavy boiling entrainer can be found more easily than intermediate boiling temperature entrainers which are interesting only if the low relative volatility between the original components is caused by a dissimilar deviation of the ideal behaviour instead of the proximity of their boiling temperature.

If the entrainer forms an azeotropic mixture with at least one of original component, azeotropic distillation process, where the entrainer is initially mixed to the original binary mixture, is then considered. A complete set of feasibility rules based on the thermodynamic and topological properties of the resulting ternary mixture has been published, whether the ternary mixture is fully miscible[1] or partially miscible with at least one unstable heterogeneous azeotrope.[2,3] In azeotropic distillation, an unstable node of the ternary system is always drawn as distillate product at the column top. On the other hand, extractive distillation process, where continuous entrainer feeding at an intermediate tray of the column defines extractive and rectifying (resp. stripping) sections, enables to recover either the unstable (resp. stable) node or the saddle original component as distillate.[4,5]

A literature survey of homogeneous extractive distillation processes was presented in part I.[6] In all cases, entrainer (E) forms no azeotrope with either (A) or (B). Before the precepts given in part I, batch extractive distillation feasibility and the first product cut was assessed by computing the composition profiles of the rectifying (resp. stripping) and extractive section, which should intersect at any time during a feasible process. Computation using the differential simplified model proposed by Lelkes et al.[7] is preferable over the discrete composition line model of Doherty and co-workers.[8] Feasibility at infinite or finite reflux (resp. reboil) operation was studied and limiting values of operating parameters (mostly reflux (resp. reboil) ratio and entrainer feed flowrate) were shown to occur for batch extractive distillation in a rectifying (resp. stripping) column.[4,5]

Earlier continuous extractive distillation studies showed how important is the univolatility line to the process feasibility and operation.[9] Indeed, part I [6] demonstrated that a homogeneous batch extractive distillation process (BED) feasibility and products can be assessed combining insights from residue curve maps and univolatility curve properties only, without any composition profile calculation. A general feasibility criterion holds for infinite reflux operation and infinite number of stages, stating that "*homogeneous batch extractive distillation of a (A) – (B) mixture with entrainer (E) feeding is feasible if there exists a residue curve connecting (E) to (A) (resp. (B)) following a decreasing (a) or increasing (b) temperature direction inside the region where (A) (resp. (B)) is the most volatile (a) or the heaviest (b) component of the mixture*". Volatility order is imposed by univolatility lines.

In part I, the thermodynamic topological structures for homogeneous extractive distillation processes were investigated by using heavy entrainers. The feasibility criterion was illustrated for the separation of azeotropic mixtures by batch extractive distillation for class 1.0-1a and 1.0-2 ternary mixtures when the entrainer does not form any new azeotrope.[10] In general, 1.0-1a class corresponds to the separation of a minimum (resp. maximum) boiling temperature azeotrope using a heavy (resp. light) entrainer and 1.0-2 class corresponds to the separation of a maximum (resp. minimum) boiling temperature azeotrope using a heavy (resp. ligth) entrainer. Using the general feasibility criterion, former studied extractive distillation processes were revisited and new product sequences were shown to exist for heavy homogeneous entrainer, never before thought of.

Among key results, it was recalled that the stability of the singular points of the extractive composition profile maps at infinite reflux and infinitesimal entrainer flowrate is the opposite of residue curve map singular points stability. When the entrainer flowrate increases, the extractive singular points (stable node or saddle, for heavy entrainer) move towards the vertex (E). Extractive singular points located on the univolatility curve at infinitesimal entrainer flowrate move along the univolatility curve until they cross a triangle edge (a stable node for 1.0-1a and a saddle for 1.0-2). Any extractive saddle point moving inside the triangle drags along an unstable extractive separatrix (starting at the unstable extractive node located near the heavy entrainer vertex) and that defines an unfeasible region for the extractive distillation process. For 1.0-1a, that happens as reflux decreases under sufficient entrainer flowrate. For 1.0-2, that happens at any reflux for each distillate. Finally, when no univolatility curve intersect the (E – product) edge, no minimum value for F_E/V exist for either A or B product.

In part II, we show that these features hold as well as the general extractive feasibility criterion for the separation of low relative volatility mixture by using a heavy entrainer that

forms no new azeotrope. That case corresponds to the zeotropic ternary diagram class 0.0-1, whatever the boiling temperature of the entrainer. Ternary diagram class 0.0-1 has a single triangular elementary cell I and all residue curves reach the stable node by passing through the sole saddle point. Hilmen et al.[10] and Kiva et al.[11] showed how unidistribution and univolatility lines affect the shape of the residue curves. Indeed, class 0.0-1 residue curves can exhibit up to two inflexion points and the ternary composition diagram can be divided in several regions where the component volatility order is different from that defined by the boiling temperature order.

From the residue curve map analysis only so far considered in the literature, the expected product by using homogeneous extractive distillation process of a class 0.0-1 mixture in a batch rectifying (resp. stripper) column is the unstable (resp stable) original component with a heavy (resp. light) entrainer.[4,5] We show that due to the occurrence of the univolatility line, the general feasibility criterion of extractive distillation predicts other products as well.

First, the thermodynamic and topological properties of the ternary diagram 0.0-1 are presented in the light of the unidistribution and univolatility lines occurence. Second, the impact of the occurrence of a univolatility line on the separation of low relative volatility mixtures using a heavy entrainer is investigated. The general feasibility criterion holds in all cases. For validation with literature, extractive and rectifying liquid composition profile maps are computed by using the simplified model of Lelkes et al.[7] described in Part I[6]. Then, the results are corroborated by rigorous simulation using ProSim Batch software.[12] Thermodynamic models and parameters for each ternary mixture are given in Table 1.

2. Thermodynamic and topological features of the ternary diagram class 0.0-1

The simplest ternary diagram class, 0.0-1, corresponds to the separation of low relative volatility mixture with either light, intermediate or heavy entrainer (E) forming no new azeotrope with (A) or (B). Reshetov and Kravchenko published statistics of the 15 experimentally reported ternary zeotropic mixtures among the 33 possible zeotropic classes.[13] The simplest zeotropic class with no univolatility line occurrence is 71.6% (Figure 1a), while four other classes with a single univolatility line, either α_{12} or α_{23}, amount for 26.4% of reported diagrams. For class 0.0-1, there is one unidistribution line related to the saddle intermediate boiling component. Two univolatility curves may also arise, rarely together (0.25% statistical occurrence), concerning the two lightest (11.6% statistical occurrence,

Figure 1b) or the two heaviest compounds (11.0% statistical occurrence, Figure 1c).[13] Other less significantly occurring diagrams display unilateral univolatility lines and are not considered here.[13]

Class 0.0-1 diagram has a single triangular elementary cell I: any residue curve reaches the stable node by passing through the saddle point, going through a maximum at crossing the unidistribution line and undergoing an inflexion point at crossing the univolatility lines if there is no unidistribution line before it reaches the corresponding unstable or stable node. So, residue curves follow a C-shape only if no volatility line exist in the ternary diagram 0.0-1. Otherwise a S-shape is expected.[11]

Any univolatilities lines changes the components volatility order. Therefore, they affects the separation of such zeotropic mixture by using light, intermediate or heavy homogeneous entrainer even if there are no azeotropic point.[6] Literature studies used traditionnal residue curve map analysis to Figure 1a case to suggest that component (A) is always drawn as the first distillate cut in a rectifying column because (A) is the unstable node of the ternary system and no distillation boundary exists. This statement is not affected by the presence of the univolatility line α_{BE} (Figure 1c) because (A) remains as the most volatile component in the new volatility order region.

However, saddle component (B) can be also drawn at the column top as the first cut by homogeneous extractive rectifying distillation when the univolatility line α_{AB} exists (Figure 1b). Indeed, if the univolatility line α_{AB} exists, both (A) and (B) satisfy the general feasibility criterion at the same time: *existence of a residue curve connecting (E) to (A) or (B) following a decreasing temperature direction in the region where the respective component is the most volatile component of the ternary mixture*.

Analogous to the analysis made in Part I[6], feasible and unfeasible regions can occur depending on the main operating parameters, the entrainer flowrate and the reflux ratio. There location are deduced from thermodynamic insights and verified from the computing of the extractive composition profile map, similar to residue curve map (rcm) analysis. They can be bounded by one or both, stable and unstable, extractive separatrices.

2.1. Class 0.0-1, diagram a: no univolatility line exist.

Figure 2 displays the ternary diagram for the class 0.0-1 when no univolatility line exists (see also Figure 1a diagram). Component (A) is the sole rcm unstable node (Figure 2a, $F_E/V = 0$) and will be the column top product under infinite reflux operation and no entrainer feeding (BED process step 1). Comparing Figure 2a and 2b ($F_E/V \rightarrow 0^+$), extractive liquid

profile map singular points are identical to residue curve map ones but with opposite stability: vertex (A) is unstable UN_{rcm} rectification and and stable $SN_{extr,A}$ extractive node; vertex (E) is stable SN_{rcm} rectification and unstable UN_{extr} extractive node; vertex of (B) is a saddle rectification and extractive singular point (S_{rcm} $S_{B,extr}$). Note that the edges (E-A), (B-E) and (A-B) are unstable, unstable and stable extractive separatrices, respectively.

At infinite reflux, as soon as the entrainer feed ratio is turned on ($F_E/V > 0$) (BED process step 2), a rectifying and an extractive column sections arise, located above and below of the entrainer feed, respectively. Then, both extractive stable node $SN_{extr,A}$ and saddle $S_{B,extr}$ move towards vertex (E) over the binary side (E-A) and (B-E) (see Figure 2c). Linking $SN_{extr,A}$ and $S_{B,extr}$, the stable extractive separatrix moves from the (A-B) edge inside the ternary diagram. All extractive profiles reach $SN_{extr,A}$ and intercept a residue curve ending at the vertex (A). Therefore, component (A) is settled at the column top during the step 2 of BED process. There is no minimum value for F_E/V because the univolatility line α_{AB} doesn't exist.

Finite reflux with entrainer feeding (Figure 2d) is the subsequent operating step 3 in a BED process and changes the location of singular points and separatrices. Similarly to diagram 1.0-1a case (see part I[6]), the saddle point $S_{B,extr}$ leaves the binary side (B-E) and moves inside the ternary diagram. It drags along the unstable extractive separatrix UN_{extr} - S_{extr} - UN'_{extr} above which lies the unfeasible region as the corresponding extractive profiles cross the (B-E) edge towards an outside stable extractive node $SN'_{extr,B}$ and no interception with the residue curve going to (A) occurs. From a composition in the feasible reagion, the still composition path moves according to the vector cone in Figure 2d and may cross the unstable extractive separatrix, preventing total recovery of component (A) from the column. Note in Figure 2d that the stable extractive separatrix remains, now linking $SN_{extr,A}$ - S_{extr} – $SN'_{extr,B}$.

At fixed F_E/V, the minimum reflux ratio for step 3 of BED process is defined when the instantaneous still composition lies into the unfeasible region. That occurs when the unstable extractive separatrix UN_{extr} – $S_{B,extr}$ - UN'_{extr} is tangent to the still path. At an adequate and fixed reflux ratio, when F_E/V increases, singular points $SN_{extr,A}$ and $S_{B,extr}$ move towards the (E) vertex while UN'_{extr} and $SN'_{extr,B}$ keep outside of the ternary diagram. Above some $(F_E/V)_{max}$ bifurcation value (not show in Figure 2), $SN_{extr,A}$ and $S_{B,extr}$ are no longer inside the triangle and all extractive profiles cross the (B-E) edge and no interception with the rectifying profile takes place anymore. Hence, the BED process becomes unfeasible for any still composition. This behaviour will be presented in the following examples of ternary mixtures.

2.2. Class 0.0-1, diagram b: α_{AB} = 1 univolatility line exist.

Figure 3 displays the 0.0-1 case when the univolatility line α_{AB} exists. Two volatility order regions occur (Figure 1b), where (A) is not always the most volatile component. The main impact is that both (A) and (B) satisfy the general feasibility criterion and can be distillated by batch extractive distillation. At infinite reflux ratio (Figure 3a, 3b, 3c), the number of extractive singular points ($SN_{extr,A}$, $S_{B,extr}$, $SN_{extr,A}$) depends on the F_E/V value and the limiting minimum or maximum values for $(F_E/V)_A$ (subscript A indicates that A is the product) and $(F_E/V)_B$ (B is the product) are set by the hypothetical interception of α_{AB} = 1 to the binary sides (E-A) and (B-E), namely $x_{P,A}$ and $x_{P,B}$.

- For (F_E/V) lower than both $(F_E/V)_A$ and $(F_E/V)_B$ (Figure 3a), $S_{B,extr}$ and $SN_{extr,A}$ exist are located similarly to the case in Figure 2c. Only component (A) can be distillated.
- As (F_E/V) increases (Figure 3b, $(F_E/V)_B < (F_E/V) < (F_E/V)_A$), $S_{B,extr}$ intersects the univolatility curve and follows it. $S_{B,extr}$ cannot continue on the (E-B) side as in Figure 3a because the univolatility line α_{AB} changes the volatility order and (B) becomes more volatil than (A). In other words, there now exists a stable extractive node relative to B ($SN_{extr,B}$ appears on and follow the (B-E) side) and (B) becomes a possible product as it satisfies the extractive general feasibility criterion. Unstable UN_{extr} - S_{extr} - UN'_{extr} and stable $SN_{extr,A}$ - S_{extr} – $SN_{extr,B}$ extractive separatrices divides the triangle, with feasible regions to distillate (A) or (B) on either side of the unstable extractive separatrix.
- Further increasing of $F_E/V > (F_E/V)_A$ (Figure 3c) moves the extractive saddle $S_{B,extr}$ to the (E-A) edge where it merges with $SN_{extr,A}$. $SN_{extr,B}$ remains and only (B) can be distillated.

The effect of finite reflux ratio (Figure 3d, 3e, 3f) is discussed in section 4.1.2, 4.2.2 and 4.3.2 respectively. It shows that the extractive feasible region no longer covers the whole triangle and can be imposed by either the stable rectifying separatrix or the unstable extractive separatrix. Exact behavior can only be assessed by computing composition profile maps using the simplified model of Lelkes et al.[7]

2.3. Class 0.0-1, diagram c: α_{BE} = 1 univolatility line exist.

As stated before the α_{BE} = 1 curve does not change the relative volatility of (A) and (B) (Figure 1c). Therefore, this case behaves similarly to the one with no univolatility curve (Figure 1a and Figure 2) as far as separation of a (A) – (B) mixture using a heavy entrainer is the issue.

3. Separation of Class 0.0-1 mixtures when no univolatility line exists.

For the simplest class 0.0-1 case when no univolatility line exist (Figure 1a), batch extractive separation of (A) – (B) by using a heavy entrainer is feasible in a rectifier as illustrated for the n-heptane (A) – toluene (B) – phenol (E)[4,14] or the benzene (A) – toluene (B) – phenol (E)[15] mixtures or in a stripper for the n-heptane (A) – toluene (B) – chlorobenzene (E) mixture.[5]

The residue curve map and composition liquid profiles map for $F_E/V = 0.5$ at infinite reflux ratio (Figure 4a) and at $R = 5$ (Figure 4b) for the ternary mixture n-heptane (A) – toluene (B) – phenol (E) studied by Lang et al.[14] and Steger et al.[4] The undistribution line $K_B = 1$ and two equivolatility lines, $\alpha_{AB} = 1.5$ and $\alpha_{AB} = 2.5$, are also shown in Figure 4a. With no univolatility line α_{AB} present, the lightest original component, n-heptane, is the most volatile component in the whole ternary composition space.

As predicted by the general extractive feasibility criterion, n-heptane is a batch extractive rectification product. Figure 4a shows that under infinite reflux and infinite number of stages, choosing a distillate x_{DA} near the n-heptane vertex $x_{DA} = \{0.98; 0.01; 0.01\}$, all extractive composition profiles reach the extractive stable node $SN_{extr,A}$ located at the n-heptane – phenol side and intersect a residue curve reaching x_{DA}. Increase of F_E/V was described in Figure 2c and no minimum value for F_E/V exists because of the absence of the univolatility line α_{AB} in the ternary diagram. Hence, the separation of n-heptane (also the residue curve unstable node) is even feasible without entrainer feeding, by azeotropic distillation.

Lang et al. showed by simulation that the extractive distillation process has a better recovery yield and distillate purity than the azeotropic distillation process because the unstable extractive separatrix is closer to the (B-E) side than the respective stable rectifying separatrix at finite reflux ratio.[14,15] Hence, the extractive feasible region (shaded area in Figure 4b) is larger than the rectifying/azeotropic feasible region. Steger et al. reached the same conclusions by computing extractive composition profiles using the differential model of Lelkes et al. and by rigorous simulation.[4,7]

Like Figure 2d, Figure 4b illustrates this for $F_E/V = 0.5$ and $R = 5$ by displaying the extractive and rectifying composition profiles maps. Setting a finite reflux moves the extractive saddle $S_{B,extr}$ inside the triangle along with an unstable extractive separatrix $UN_{extr} – S_{B,extr} – UN'_{extr}$ that defines the shaded extractive feasible region but also prevents the complete recovery of n-heptane. This behavior is similar to the case studied in part I[6] for the separation of minimum azeotropic mixtures using heavy entrainer (class 1.0-1a).

Again, the rectifying separatrix splits the diagram in two regions, one being feasible for azeotropic distillation to reach x_{DA}, the other to reach a hypothetical distillate near B.

Again, the extractive and rectifying feasible regions interfer to obtain x_{DA}. At R = 5, the rectifying/azeotropic feasible region is smaller than the extractive feasible region, leading to the concluding comments in the literature recalled above.

Another illustration is provided by the separation of the n-heptane (A) – toluene (B) mixture using heavy chlorobenzene (E). It was studied by Varga considering a batch extractive stripper but with lesser performance than the rectifier conFiguration.[5] If we consider extractive rectification for this system, the overall behavior is similar to the previous n-heptane – toluene – phenol case, but differs at finite reflux.

The thermodynamic and topological characteristics of the ternary mixture are shown for $F_E/V = 0.5$ in Figure 5a along with equivolatility lines, α_{AB} = 1.5 and α_{AB} = 2, the undistribution line K_B = 1, rectifying and extractive composition profiles maps under infinite reflux and x_{DA}. Under infinite reflux, any composition is feasible as all extractive profile reach an extractive stable node $SN_{extr,A}$ at the (A–E) edge and can intersect a residue curve reaching x_{DA} (Figure 5a).

Under finite reflux, the stable rectifying and the unstable extractive separatrices move inside the triangle (Figure 5b). Compared to Figure 4b mixture, the stable rectifying separatrix is not closer but farther from the (E-A) edge than the unstable extractive separatrix. So, the feasible region is below the stable rectifying separatrix (shaded region) where interception between an extractive and a rectifying composition profile leading to x_{DA} takes place. In particular that concerns the area between both separatrices where extractive composition profiles may cross feasible rectifying profiles provided that the number of trays in the extractive section is below a $N_{A,MAX}$ to avoid extractive composition to end in the unfeasible rectifying region.

All this shows that under finite reflux, location of singular point and separatrices location, by computing extractive and rectifying composition profiles, are needed to investigate feasibility.

Comparing the separation of n-heptane (A) – toluene (B) with different entrainers (E), phenol (Figure 4) or chlorobenzene (Figure 5) (we have used the same thermodynamic model and binary parameters for the mixture (A)-(B), see table 1, and the same product purity), the equivolatility lines in Figure 5a and 4a show that phenol enhances the relative volatility α_{AB} more than chlorobenzene. This affects the performance of the extractive process as the extractive saddle $S_{B,extr}$ is located closer to the unstable extractive node UN_{extr} at infinite reflux ratio for chlorobenzene (Figure 5a) than for phenol (Figure 4a). Besides, under the same finite

reflux, F_E/V and target x_{DA} values, chlorobenzene brings an unstable separatrix that sets a smaller feasible region for separating n-heptane than phenol (Figure 4b and 5b).

For both ternary mixtures, the feasible region can be enlarged by increasing the reflux ratio, thus improving the recovery yield of n-heptane. Driving the still composition and adjusting the reflux policy is a typical advantage of batch distillation over continuous distillation. Indeed, the still composition path moves within a composition region under imposed reflux and entrainer flowrate conditions according to the vector cone determined by the addition of E and away from the distillate D_A (Figure 4b and 5b).

As in part I[6], recommanded operation is to start at low reflux and then to increase it. Initial reflux should not be too low so that the unstable extractive separatrix [UN_{extr} – $S_{B,extr}$ – UN'_{extr}] starts close to the entrainer vertex providing a better recovery of n-heptane. A maximum recovery of 99% for n-heptane (unstable separatrix intersecting the (E-A) edge at {0.01; 0.00;.099}) is achieved under $F_E/V = 0.5$ with $R = 2.6$ for phenol and $R = 36$ for chlorobenzene). If the still composition x_S crosses the unstable extractive separatrix, and leaves the feasible region to obtain x_{DA}, the top product will shift from x_{DA} to a product likely located near (B). So, as x_S nears the unstable extractive separatrix, it is recommanded to increase the reflux ratio in order to expand the extractive feasible region and continue to obtain high purity n-heptane while keeping the overall n-heptane recovery yield high.

Overall, from the mixture thermodynamic features, phenol is a better entrainer than chlorobenzene: less entrainer consumption, low reflux ratio for the same recovery yield; inducing less heat duty and a smaller column.

4. Separation of Class 0.0-1 mixtures when α_{AB} univolatility line exists.

We consider the separation of ethyl acetate (A) – benzene (B) with n-hexanol (E). and compute the residue curve map by using UNIFAC thermodynamic model (Figure 6). Azeotropic rectification to recover ethyl acetate is feasible but costly because the low mixture average relative volatility of 1.12 implies a high number of stages and reflux ratio. The unidistribution line for benzene (K_B) lies close to the binary side (A-B). The univolatility line α_{AB} intersects both the (E-B) and (E-A) edges and divides the composition space in two volatility order region of similar size: one where benzene (B) is more volatil than ethyl acetate (A) despite having a boiling point higher than (A); the other where (A) is more volatil than (B) (Figure 6). In each region a residue curve goes from vertex (E) to (A) or (B) following a

decreasing temperature direction. So, both (A) and (B) satisfy the general extractive feasibility criterion and are possible products under infinite reflux condition.

To confirm these precepts by computing composition profiles, two product cuts rich in (A) or (B) are defined, x_{DA} = {0.98, 0.01, 0.01} and x_{DB} = {0.01, 0.98, 0.01}. First considering x_{DA}, we use the analysis made in section 2 and Figures 2 and 3. For infinite reflux and $F_E/V \rightarrow 0^+$, a stable extractive node $SN_{extr,A}$ lies in (A) whereas (B) is an extractive saddle point $S_{B,extr}$ (Figure 2b). As F_E/V increases, $SN_{extr,A}$ moves along the (E–A) edge until it reaches $x_{P,A}$, hypothetical intersection of $\alpha_{AB} = 1$ and (E–A) edge (Figure 3a). Recovering (A) with purity x_{DA} is possible until F_E/V reaches a maximum value $(F_E/V)_{maxA}$ for which $SN_{extr,A}$ lies in x_{PA}. Above $(F_E/V)_{maxA}$, $SN_{extr,A}$ no longer exists and (A) cannot be obtained by extractive distillation. Dissimilar behaviour is observed for component (B) that is recovered only if F_E/V is greater than a minimum value $(F_E/V)_{minB}$ for which $S_{B,extr}$ lies on x_{PB}. Below $(F_E/V)_{minB}$, $SN_{extr,B}$ does not exist. Above, it does and (B) can be obtained by extractive distillation (Figure 3b and 3c). As seen in Figure 3b there might exist a F_E/V range for which both $SN_{extr,A}$ and $SN_{extr,B}$ exist and (A) and (B) can be distillated depending on the location of the still composition in the ternary diagram.

The existence of maximum or minimum entrainer flowrate value depends then on the occurrence of univolatility lines under infinite reflux operation. Determination of their precise values requires computation of extractive profiles nodes location, either from extractive profile maps, as we do or from finding the roots and turning points of the differential set of equation by interval analysis [17] or by bifurcation analysis [18].

Finite reflux operation is discussed below and impacts significantly the possible products: whatever the entrainer flowrate, both (A) and (B) are candidate product because separatrices move inside the triangle at finite reflux due to the removal of one product and they set feasible and unfeasible regions. Care should be taken to prevent the still composition to cross into the unfeasible region, provoking a suddent change in product.

4.1. Low entrainer flow rate $F_E/V < \{ (F_E/V)_{maxA} ; (F_E/V)_{minB} \}$

4.1.1. Infinite reflux operation: (A) is the only possible distillate. Figure 7a displays the extractive composition profiles map at infinite reflux considering F_E/V lower than both $(F_E/V)_{maxA}$ and $(F_E/V)_{minB}$. As expected from Figure 3a, Only $SN_{extr,A}$ exists and x_{DA} is obtained whatever the still composition: all extractive composition profiles end on the binary side (A – E) at the stable extractive node $SN_{extr,A}$ and cross a residue curve reaching x_{DA}. With no impact on the feasibility, a stable extractive separatrix links $SN_{extr,A}$ coming from (A) and the saddle extractive point $S_{B,extr}$ coming from the saddle vertex of (B). Note that ethyl acetate (A) is also

the sole residue curve map unstable node of the ternary system and this component goes to the column top even at infinite reflux without entrainer feeding (this is azeotropic distillation). The feeding of n-hexanol changes the liquid composition profile inside the column, enabling to link the punctual still composition to the top product x_{DA} through a combination of extractive and rectifying section.

4.1.2. Finite reflux operation: (A) and (B) are possible distillate. As expected from Figure 3d, a stable rectifying separatrix appears under finite reflux even for a class 0.0-1 ternary system that doesn't exhibit a residue curve boundary. Depending on the composition location on a side or other of the rectifying separatrix, rectifying profile reach either the (B) vertex or the (A) vertex vicinity. Besides, an unstable extractive separatrix [$UN_{extr} - S_{B,extr} - x_{UN}$] is dragged along as $S_{B,extr}$ moves inside the triangle. Figure 7b shows the rectifying and extractive composition profiles maps for R = 50, F_E/V = 0.1 computed for a distillate x_{DA}. UN_{extr} is close to the (E) vertex and x_{UN} is the intersection point of the unstable extractive separatrix with the (A–B) edge. Extractive separatrices intersect at the ternary extractive saddle $S_{B,extr}$. As usual in the extractive distillation process with heavy entrainers (see part I[6]) the unstable extractive separatrix generates unfeasible and feasible regions to recover x_{DA}. However interference with the stable rectifying separatrix now arise. Indeed, the feasible region is the composition area where combined extractive section and rectifying section profiles enable to recover x_{DA}. That happens below the unstable extractive separatrix for any extractive section composition. That also happens in the area between the unstable extractive and the stable rectifying separatrices. There lies the extractive composition if the number of theoretical trays in the extractive section is below a $N_{A,max}$ value and it can intersect the rectifying profiles reaching x_{DA} (Figure 7b).

Note that even for R = 50, total recovery of ethyl acetate is not achievable because the stable rectifying separatrix is located far enough of the benzene – n hexanol edge. The scenario gets worst for lower value of the reflux ratio for both alternatives, azeotropic and extractive batch distillation process.

The separation of ethyl acetate by extractive distillation process for F_E/V = 0.1 and R = 50 is verified by rigorous simulation using ProSim Batch program and considering the following column features: total number of equilibrium stages (N_T = 90), n-hexanol is fed at the tray 20 from the top, total condenser, adiabatic column; negligible liquid holdup and no pressure drop. The initial binary mixture composition (x_{S0}) is located inside the feasible region below the unstable extractive separatrix. The simulation entrainer and the vapour flowrates are defined to give an approximate value of F_E/V = 0.1 inside the extractive column section.

Figure 8 shows the simulation results such as the still path and the liquid composition profile inside the column for four different periods: (period 1, circle, $F_E/V = 0.1$ and $R \infty$) operation at infinite reflux with continuous feeding of n-hexanol during 0.5h (x_{S1}); (period 2, shaded square, $F_E/V = 0.1$ and $R = 50$) the still path reaches the unstable extractive separatrix at x_{S2}; (period 3, white square, $F_E/V = 0.1$ and $R = 50$) the still path (x_{S3}) reaches the stable rectifying separatrix at x_{S3} and (period 4, lozenge, $F_E/V = 0.1$ and $R = 50$) the composition of ethyl acetate into the still is equal to 0.01 (x_{Sf}) and the distillation process is stopped.

All extractive and their respective rectifying liquid composition profile intersect very close to the stable extractive separatrix (interception point I_1, I_2, I_3 and I_f in Figure 8). After step 1 ($F_E/V > 0$, R∞), I_1 almost reaches $SN_{extr,A}$ on the ethyl acetate – hexanol edge (theoretically, it would with an infinite number of equilibrium trays in the extractive section) and ethyl acetate remains into the condenser nearly pure (x_{DA1}). As distillate removal starts with $R = 50$, the distillate purity is maintained but it drops (x_{DA2} near 90% of A) when the still path comes near the unstable extractive separatrix at x_{S1}. That happens because the number of equilibrium trays in both column sections is large but not enough. This situation deteriorates as the still path moves towards the binary side benzene – hexanol: interception points I_2, I_3 and I_f moves on the stable extractive separatrix towards the stable extractive node $SN_{B,extr}$ and the distillate purity corresponding to the end of the rectifying section profile decreases significantly from x_{DA2} to x_{DAf}. As shows the I_f location in Figure 8, the extractive liquid composition profile direction is reversed when the still path crosses the stable rectifying separatrix to go into the unfeasible region.

To conclude on this example, separation of ethyl acetate is possible as predicted but the purity is not good at such a low F_E/V ratio despite a large number of trays and an elevated reflux ratio.

4.2. Medium entrainer flow rate $(F_E/V)_{min,B} < F_E/V < (F_E/V)_{max,A}$

4.2.1. Infinite reflux operation: (A) and (B) are possible distillate. For $F_E/V = 0.5$ between $(F_E/V)_{minB}$ and $(F_E/V)_{maxA}$, both extractive stable nodes $SN_{extr,A}$ and $SN_{extr,B}$ exist even at infinite reflux and both (A) and (B) are possible distillates. Similarly to the behaviour shown in Figure 3b, the extractive composition profiles map exhibits four extractive separatrices crossing at the ternary extractive saddle point $S_{B,extr}$, that is located on the univolatility line ar infinite reflux. Depending on the still composition on a side or the other of the unstable extractive separatrice $UN_{extr} - S_{B,extr} - UN'_{extr}$, either ethyl acetate or benzene goes up to the column condenser because extractive composition profile arriving to $SN_{extr,A}$ or $SN_{extr,B}$ intersect a residue curve reaching x_{DA} or x_{DB}.

This is verified by rigorous simulation using ProSim Batch program and considering the following column features: total number of equilibrium stages (N_T = 90), n-hexanol fed at tray 10, total condenser, adiabatic column; negligible liquid holdup and not pressure drop. The entrainer and the vapour flowrates were defined to give an approximate value of F_E/V = 0.5 inside the extractive section. Two initial charge compositions, x_{S1} and x_{S2}, are located below and above the unstable extractive separatrix. Figure 9 display the still path and the liquid composition profile inside the column after 0.5hr of infinite reflux operation with continuous feeding of n-hexanol (step 2 of BED). Simulation results match very well liquid composition profiles computed by the simplified model. Concerning the distillate purity, the elevated number of trays in the extractive section (80) is not enough to obtain from x_{S1} the 98% ethyl acetate purity composition expected in the simplified analysis (Figure 7). However more than 98% benzene is obtained from x_{S2}. In that case ethyl acetate (unstable node) that first settled at the condenser when the column is started up at infinite reflux without entrainer feeding (step 1 of BED) is replaced by benzene during the 0.5hr of n-hexanol feeding under infinite reflux.

4.2.2. Finite reflux operation: (A) and (B) are possible distillate. As expected from Figure 3e, Keeping F_E/V = 0.5 at finite reflux does not change qualitatively the process but now the extractive separatrices no longer intersect on the univolatility line. Furthermore, finite reflux means that either x_{DA} or x_{DB} distillate is removed. Then composition profile maps must be computed considering either either x_{DA} (Figure 10a) or x_{DB} (Figure 10b), setting R = 20. In both cases, the feasible extractive region is smaller than at infinite reflux (Figure 9) because the unstable extractive separatrix comes closer to the distillate location as the column is depleted from the distillate. This is particularly significant for ethyl acetate distillation. Operation at finite reflux has also affects rectifying composition profiles. Only in the case of ethyl acetate distillate removal, the stable rectifying separatrix exists, emerging from the (E/SN_{rcm}) – (B/S_{rcm}) edge towards the. As before the stable rectifying separatrix sets the shaded feasible region where extractive composition profile intercept rectifying composition profile reaching x_{DA} (Figure 10a).

In the case of benzene distillate removal, the stable rectifying separatrix that was located on the (E/SN_{rcm}) – (B/S_{rcm}) edge under infinite reflux cannot move under finite reflux closer to the distillate than it was under infinite reflux and thus doesn't exist. The shaded feasible region is set by the unstable extractive separatrix (Figure 10b). A closer look at the rectifying composition profiles shape in Figure 10b indicates that at the chosen reflux, high purity benzene recovery will be very tricky: the shape is more curved at R = 20 than at infinite reflux (compare with Figure 6). Hence, a high number of trays in the extractive column section will

be required in order for both section composition profiles to intercept as close as possible to the (B-E) edge. Otherwise, extractive profile will intersect rectifying profiles going first to the binary side (A-B) and the distillate product will be always polluted with (A).

Performance of the separation of ethyl acetate and benzene at finite reflux ratio was verified by rigorous simulation using ProSim Batch under the same simulation condition than before and for the same initial still compositions, x_{S1} and x_{S2}. Extractive and rectifying composition profiles are shown in Figure 11, computed from the still compositions obtained after the 0.5hr of infinite reflux operation (x_{S01} and x_{S02}) for R = 20 keeping the entrainer feeding (step 3 of BED) at different times. At x_{S01} and x_{S02}, the extractive and rectifying composition profiles coincides with those shown in Figure 9 and the purity of ethyl acetate (x_{DA}) and benzene (x_{DB}) are similar to those in Figure 9. After 10 min of extractive distillation with R = 20, the still composition lie in $x_{S1'}$ and $x_{S2'}$ and the distillate purity ($x_{DA'}$ and $x_{DB'}$) diminishes significantly. After 3 hr, x_{S1f} and x_{S2f} are the still compositions and the distillate purity (x_{DAf} and x_{DBf}) has remained close to $x_{DA'}$ and $x_{DB'}$. The ethyl acetate and benzene average distillate purity is around of 80% and 86%, respectively. The 98% x_{DA} and x_{DB} distillate purity is not achieved in both cases as expected because x_{S01} and x_{S02} and their respective still path ($x_{S1'}$ to x_{S1f} and $x_{S2'}$ to x_{S2f}) are located inside the unfeasible region predicted by the simplified model (see Figure 10a and 10b). Also, as predicted in Figure 10, finite reflux ratio operation in the unfeasible region changes the extractive liquid composition profile shape for $x_{S1'}$ and x_{S1f} , pointing first towards the opposite side of the location of $SN_{extr,A}$ for the case of ethyl acetate instead of towards $SN_{extr,A}$. For separating benzene, the extractive composition profile intercepts the rectifying composition profile far enough from the binary side (B-E) despite the high of number of extractive equilibrium trays (80). In both cases, the still path is almost linear towards the entrainer composition vertex due to the elevated reflux ratio and the low purity of the distillate products. The still path follows a vector cone displayed for $x_{S1'}$ and $x_{S2'}$, contribution of $x_{Entrainer}$ and the instantaneous distillate purity ($x_{DA'}$ and $x_{DB'}$) (Figure 11). Improving the distillate purity for both original components can be only achieved by increasing the reflux ratio. A higher reflux ratio will notably shift the unstable extractive separatrix away from the stable nodes $SN_{extr,A}$ and $SN_{extr,B}$, increasing the feasible region size for ethyl acetate and benzene, respectively.

4.3. High entrainer flow rate $\{ (F_E/V)_{max,A} ; (F_E/V)_{min,B} \} < F_E/V$

4.3.1. Infinite reflux operation: (B) is the only possible distillate. For F_E/V higher than $(F_E/V)_{minB}$ and $(F_E/V)_{maxA}$, only $SN_{extr,B}$ exists inside the composition space and benzene (B) can be drawn as first distillate cut (Figure 12 is drawn for F_E/V = 2). The stable extractive

separatrix joins the saddle $S_{B,extr}$ and the stable node $SN_{extr,B}$. Hence, the topological structure of the extractive profile map corresponds to that shown in Figure 3c. In the absence of an unstable extractive separatrix, for any composition an extractive composition profile exists, ending at the extractive stable node $SN_{extr,B}$ and intercepting the selected residue curve which goes through the desired distillate purity at x_{DB}. Simulation results using ProSim Batch considering F_E/V = 2 and infinite reflux are displayed in Figure 12 as well. A distillation column with 90 theoretical stages is considered with the entrainer fed at tray 10. The vapour flowrate generated at the boiler is defined in order to provide an approximately ratio of F_E/V = 2 inside the extractive column section. When the column is started up at infinite reflux (step 1 of BED), the steady state liquid composition profile almost reaches the ethyl acetate vertex (see $x_{DA\infty}$ in Figure 12). Entrainer feeding under infinite reflux is then performed until the benzene is settled into the condenser with the expected molar purity of 98% (x_{DB}). IN the mean while, the still path has followed a rectilinear trajectory toward the entrainer vertex. The simulated extractive and rectifying section composition profiles match the simplified model predictions and intercept close to $SN_{extr,B}$.

4.3.2. Finite reflux operation: (A) and (B) are possible distillate. As expected in Figure 3f, Figure 13 shows for R = 50 and F_E/V = 2 that under finite reflux ratio operation, the extractive saddle $S_{B,extr}$ now moves inside the triangle, bringing along an unstable extractive separatrix $UN_{extr} - S_{B,extr}$ - UN'_{extr} that splits the triangle into two distinct feasible region for recovering benzene (B) or ethyl acetate (A), much like what was found for the case $(F_E/V)_{\min B} < (F_E/V) < (F_E/V)_{\max A}$ (Figure 3b and Figure 10b). That happens because in each region extractive composition profiles reach either $SN_{extr,B}$ or $SN_{extr,A}$ that are located close to the (E-B) or (E-A) edges respectively. Figure 13 also displays the rectifying liquid composition profile going through x_{DB} = (0.01, 0.98, 0.01). It is similar to residue curves showed in Figure 6 because of the high reflux ratio (R = 50). Hence, no rectifying boundary exists and the feasibility of the separation of benzene is mostly determined by the unstable extractive separatrix $UN_{extr} - S_{B,extr}$ - UN'_{extr}.

Considering a still composition into the feasible region I for recovering (B), the still path direction is governed by the vector cone addition of (E) and removal of (B). that may bring the still composition across the unstable extractive separatrix. As a consequence, the distillate will be polluted quickly with the ethyl acetate as the extractive profile will rapidly end near $SN_{extr,A}$ instead of $SN_{extr,B}$. The opposite will happen if x_S is in the feasible region II.

Figure 14a and 14b show rigorous simulation results with the same column features as before for x_S compositions located in the feasible region I (x_{S10}) and II (x_{S20}) respectively.

Starting from x_{S10} into feasible region I, x_{S11} is reached after infinite reflux and entrainer feeding operation (step 1 of BED followed by step 2). Composition profiles match the previous infinite reflux simulation, settling first ethyl acetate in the condenser and replacing it by benzene – rich distillate x_{DB} thank the entrainer feeding (see Figure 12 and Figure 14a). As distillate removal proceeds (step 3 of BED), the vector cone motion of the still composition is almost rectilinear towards the entrainer vertex because of the high reflux ratio. The instantaneous distillate purity is maintained above 98% of benzene ($x_{DB,I}$) for the still path going from x_{S1} to x_{S12}. The composition profiles are display in Figure 14a for $x_{S1'}$, ten minutes after x_{S1} and for the last time when 98% benzene purity is achieved (x_{S12}). Composition profiles agree well with those of the simplified model with an interception between rectifying and extractive composition profiles taking place at x_I located near $SN_{extr,B}$. Note that the still composition x_{S12} is very close to the unstable extractive separatrix. Then distillate removal is continued until the composition of benzene into the still remains less than 1% (x_{S1f}). This removal brings the still composition across the unstable extractive separatrix, resulting in the pollution of the distillate with ever more ethyl acetate, decreasing until 88% ($x_{DB,II}$ path).

Now, we consider starting from x_{S20} into region II. Under infinite reflux with no entrainer feeding (step 1 of BED), the liquid composition profile links x_{S02} to ethyl acetate at $x_{DA\infty}$ following usual non extractive distillation rules as ethyl acetate; the residue curve unstable node; is obtained into the condenser. Feeding n-hexanol (step 2 of BED) under infinite reflux brings benzene (x_{DB1}) instead of ethyl acetate at the column top because at infinite reflux ratio the whole ternary diagram is feasible for the separation of benzene (see Figure 12). At the end of this step 2, the still lies in x_{S21}. When distillate removal starts with R = 50, the distillate composition changes abruptly, lying in $x_{D'}$ after two minutes (75% of benzene) and $x_{D''}$ after ten minutes (46% of benzene) for which the whole composition profile is shown in Figure 14b. The simplified model predicted that the still composition being in the region II, ethyl acetate should be obtained in the distillate. However, In simulation, one observes a rapid but not instantaneous increase of ethyl acetate in the distillat because of the column composition inertia, in particular the fact that it lies after step 1 in region I. R = 50 distillate removal is carried out until the still composition in benzene is less than 1% (x_{S2f}). The corresponding composition profile is shown and the distillate composition has move closer to ethyl acetate.

In summary, the withdrawal of ethyl acetate or benzene is possible by feeding n-hexanol depending on the value of F_E/V because the univolatility line α_{AB} divides the composition space in similar feasible regions for component (A) and (B).

However, the extractive separation of ethyl acetate may become more difficult when the univolatility line α_{AB} lies closer to the binary side (A-B), decreasing the region wherein component (A) is the most volatil. That is the case of the separation of the same binary mixture ethyl acetate – benzene when 1-butanol is used as heavy entrainer. The residue curve map is shown in Figure 15 using UNIQUAC as thermodynamic model. In this case, $\alpha_{AB} = 1$ is located close to the binary side ethyl acetate – benzene. One notes in Figure 15 that there is a minimum value of F_E/V for recovering component (B) ($(F_E/V)_{minB}$) given by the hypothetical interception (x_{PB}) of the univolatility line at the binary side (B-E). Besides, because of the location of the interception point (x_{PA}) of $\alpha_{AB} = 1$ at the edge (E-A) very close to the vertex (A), the maximum value F_E/V ($(F_E/V)_{maxA}$) for recovering component (A) under infinite reflux is almost zero. Therefore, benzene is easier to recover than ethyl acetate by homogeneous extractive distillation. Comparing Figure 15 and Figure 3, the ethyl acetate – benzene – 1-butanol mixture has a slightly different process behavior because of the particular shape of the univolatiliy line that sets the x_{PA} farther from (E) than the x_{PB} point on their respective (E-A) and (E-B) edges. The opposite holds in Figure 3. We now discuss the impact on the process operation.

Figure 16a displays the extractive composition profile map for $(F_E/V) = 0.1$ at infinite reflux operation. At such a low entrainer feed flowrate, $(F_E/V)_{maxA} < (F_E/V) < (F_E/V)_{minB}$ (A) can no longer be recovered and (B) cannot be recovered yet: $SN_{extr,A}$ does not exist and for x_{DB} = (0.01;0.98;0.01) the extractive stable node $SN_{extr,B}$ is located on the univolatility line (precisely on the line under infinite reflux) and all extractive composition profiles finish at this point where a rectifying profile cannot reach x_{DB}. The extractive liquid composition profiles map also exhibits stable extractive separatrices joining $SN_{extr,B}$ to the two extractive saddle points $S_{A,extr}$ and $S_{B,extr}$ placed on the binary side (E-A) and (B-E), respectively. This is a behavior similar to the one discussed in Part I for the separation of a minimun boiling azeotrope when $(F_E/V)<(F_E/V)_{min}$. as in part I, to recover (B) a higher (F_E/V) must be used in order to locate $SN_{extr,B}$ on the binary side (B-E) between the point x_{PB} and the vertex (E). That happens for $F_E/V = 0.5$ at infinite reflux (Figure 16b). Whatever the still composition, the extractive stable node $SN_{extr,B}$ is now located on the binary side (B-E) and can cross the residue curve reaching x_{DB}. Note under such a high (F_E/V), the extractive singular node map with an extractive stable node $SN_{extr,B}$ and and extractive saddle $S_{A,extr}$, is similar to that sketched in Figure 3c. The process behavior will then be similar to that observed for Figure 3c case (see section 4.3): Figure 16b matches Figure 12 features under infinite reflux.

At finite reflux ratio (Figure 17 for for $F_E/V = 0.5$, $R = 30$ and $x_{DB} = (0.01;0.98;0.01)$), an unstable extractive separatrix UN_{extr} - S_{extr} - UN'_{extr} appears because $S_{A,extr}$ goes inside the composition space, similar to features displayed in Figure 13. Hence, there is also a stable extractive separatrix linking $SN_{extr,B}$, S_{extr} and $SN_{extr,A}$. The stable node $SN_{extr,A}$ is placed near but below the (E-A) edge. Above (resp. below) the unstable extractive separatrix (region I) (resp. (region II)) all extractive liquid composition profiles go to the binary side (E-B) (resp. (E-A)) and intercept a residue curve going to (B) benzene (resp. (A) ethyl acetate) that can be recovered as distillate. At such a high reflux ratio ($R = 30$) rectifying composition profiles are not displayed in Figure 17 as they are very close to residue curves Further more, no rectifying separatrix exists and the feasible regions are only determined by the presence of the unstable extractive separatrix. Finally, complete recovery of benzene is not possible under these operating conditions because the still composition x_S will be forced to cross the unstable extractive separatrix due to the combined effect of feeding the entrainer x_E and the withdrawal of benzene x_{DB} (see Figure 17 cone of motion). In that case, distillate product will be polluted with ethyl acetate when the still composition lies inside region II. A solution to improve recovery would be to increase the reflux ratio (e.g. $F_E/V = 2$) to move closer the unstable extractive separatrix to the binary side ethyl acetate – n butanol and expand the feasible region I for recovering benzene by extractive distillation.

To validate this simplified model analysis, Figure 18 displays rigorous simulation by using ProSim Batch (ProSim S.A). The initial still composition (x_{S0}) is equimolar in benzene and ethyl acetate. The vapour overflow leaving the reboiler and the feeding of the n-butanol is defined for obtaining approximately $F_E/V = 0.5$. The column has 80 equilibrium stages and the entrainer is fed at tray 10 from the top. The same operating ideal conditions considered in the previous simulation are kept. The batch column is started up at infinite reflux (step 1 of BED) and the liquid composition profile inside the column links x_{S0} to near ethyl acetate, the residue curve unstable node of the original binary mixture. Showing how low is the relative volatility of benzene - ethyl acetate, 80 trays are not sufficient to get better than 93% of ethyl acetate in the condenser composition $x_{DA\infty}$. As entrainer feeding starts under infinite reflux (step 2 of BED), benzene replaces ethyl acetate in the condenser with a molar purity of 98.5% (x_{DB}) while the still composition moves from x_{S0} to x_{S1} towards the entrainer n-butanol vertex (*EFeed* path in Figure 18). The composition profile connects x_{S1} to x_{DB} by means of two extractive and rectifying composition profiles that intersect close to the stable node $SN_{extr,B}$ computed by the simplified method. Once x_{DB} distillate removal starts (step 3 of BED) under $R = 30$, the still path is influenced by the combined contribution of the feeding of n-butanol

(x_E) and the withdrawal of benzene (x_{DB}) according to Figure 18, hinting that it might cross the unstable extractive separatrix. That happens when the still composition lies in x_{S2}. While the still path moves from x_{S1} to x_{S2}, benzene average purity in the distillate reaches 98%, decreasing along the distillate composition path (x_{DB1}) (Figure 18). This deacrease is attributed to the finite size of the column and the overall depletion of benzene in the column. Once the still path crosses the unstable extractive separatrix, benzene purity in the distillate decreases quickly along the distillate path (x_{DB2}) on the binary side ethyl acetate – benzene, ending at 63.4% of benzene. That is what the simplified model predicted. However, the final benzene composition into the still is lower than 0.01 and the final average distillate purity in benzene still reach 97.3%. Improvement of the recovery yield and the purity of benzene could have been achieved if the reflux ratio was increases to moves the unstable extractive separatrix towards to ethyl acetate – n-butanol edge, increasing the feasible region enabling to achieve better than 98% distillate purity.

5. Conclusion

Synthesis and design of the separation of low relative volatility by batch extractive distillation using heavy entrainers is not as simple as past studies thought of. Occurence of the univolatility line α_{AB} inverses the (A)-(B) relative volatility and both compounds can be distillated depending on the entrainer feed and reflux conditions. Under infinite reflux, identification of the original component to be drawn as the first distillate cut is always achieved without tedious calculations by considering the general extractive distillation feasibility criterion enounced in part I: *there is a residue curve going from the entrainer vertex to (A) or (B) following a decreasing temperature direction inside the region in which (A) or (B) is the most volatile component.* Limit values of entrainer feed flowrate are deduced from the extractive profile map. Finite reflux operation can be roughly predicted but requires more detailled calculations.

As previously known, when no univolatility line exist (71.6% statistical occurrence among 0.0-1 class diagram), the light original component (residue curve map unstable node) (A) is drawn as distillate product. Two heavy entrainers (E), phenol and chlorobenzene, were compared for the separation of n-heptane (A) – toluene (B) and it was observed that the α_{AB} relative volatility increase was greater for phenol than for chlorobenzene and that the corresponding batch extractive process was in theory more efficient, enabling a better recovery yield with less entrainer consumption and reflux than for chlorobenzene.

Both univolatility line α_{AB} and α_{BE} can occur, rarely together (0.25% statistical occurrence). When the univolatility line α_{BE} occurs (11.0% statistical occurrence) the extractive process behaves like when no univolatility line exist. However, when the univolatility line α_{AB} exists, it changes the (A) – (B) volatility order in one region as (B) becomes more volatil than (A) and can be also recovered as first distillate cut. Which product (A) or (B) is recovered depends on the reflux condition and on the still composition location. Illustration is provided for several 0.0-1 mixtures: feasibility predictions are discussed, then confirmed by composition profile maps calculations and further by rigourous simulations.

Under infinite reflux operation, the entrainer flow rate value affects the occurrence of extractive stable nodes for (A) or (B) in relation with the intersection of the univolatility line α_{AB} with the triangle edges. There exists no minimum but a maximum entrainer flow rate value for (A) to be a possible product. There exist a minimum but no maximum entrainer flow rate value for (B) to be a possible product. Evidently some entrainer flow rate value enable to obtain either (A) or (B) depending on the still composition location.

Finite reflux operation impacts significantly the possible products: whatever the entrainer flowrate, both (A) and (B) are candidate product because unstable separatrices arise inside the triangle at finite reflux due to the removal of one product.

When conditions are suitable for both compounds to be possible products, care should be taken to prevent the still composition to cross the unstable separatrix because that leads to a suddent change in product and to a non monotoneous distillate temperature evolution.

Separation using light entrainers in a stripper column are under investigation and will confirm the usefullness of the general extractive feasibility criterion.

Literature Cited

(1) Rodríguez-Donis, I.; Gerbaud, V.; Joulia, X. Entrainer Selection Rules for the Separation of Azeotropic and Close Boiling Point Mixtures by Homogeneous Batch Distillation. *Ind. Chem. Eng. Res.* **2001**, *40*(12), 2729-2741.

(2) Rodríguez-Donis, I.; Gerbaud, V.; Joulia, X. Heterogeneous Entrainer Selection Rules for the Separation of Azeotropic and Close Boiling Point Mixtures by Heterogeneous Batch Distillation. *Ind. Chem. Eng. Res.* **2001**, *40*(22), 4935-4950.

(3) Skouras, S.; Kiva, V.; Skogestad S. Feasible Separations And Entrainer Selection Rules for Heteroazeotropic Batch Distillation. *Chem. Eng. Sci.* **2005**, *60*(11), 2895-2909.

(4) Steger, C.; Varga, V.; Horvath, L.; Rev, E.; Fonyo, Z.; Meyer, M.; Lelkes, Z. Feasibility of Extractive Distillation Process Variants in Batch Rectifier Column. *Chem. Eng. Process.* **2005**, *44*, 1237-1256.

(5) Varga, V. Distillation Extractive Discontinue dans une Colonne de Rectification et dans une Colonne Inverse. *Ph.D. Thesis*, Toulouse. **2006**.

(6) Rodríguez-Donis, I.; Gerbaud, V.; Joulia, X. Thermodynamic Insights on the Feasibility of Homogeneous Batch Extractive Distillation. I. Azeotropic Mixtures and Heavy Entrainer. Submitted to *Ind. Chem. Eng. Res*. **2008.**

(7) Lelkes, Z.; Lang, P.; Benadda, B.; Moszkowicz, P. Feasibility of Extractive Distillation in a Batch Rectifier. *AIChE J.* **1998**, *44*, 810-822.

(8) Widagdo S.; Seider W.D. Azeotropic Distillation. *AIChE J.* **1996**, *42*, 96-126.

(9) Laroche, L.; Bekiaris, N.; Andersen, H.W.; Morari, M. Homogeneous Azeotropic Distillation:Comparing Entrainers. *The Can. J. Chem. Eng.* **1991**, *69*, 1302-1319.

(10) Hilmen, E. K.; Kiva, V. N.; Skogestad, S. Topology of Ternary VLE Diagrams: Elementary Cells. *AIChE J*. **2002**, *48*(4), 752–759.

(11) Kiva, V.N.; Hilmen, E.K.; Skogestad, S. Azeotropic Phase Equilibrium Diagrams: A Survey. *Chem. Eng. Sci.* **2003**, *58*, 1903-1953.

(12) ProSim S.A. *http://www.prosim.net*

(13) Reshetov, S.A.; Kravchenko S.V. Statistics of Liquid-Vapor Phase Equilibrium Diagrams for Various Ternary Zeotropic Mixtures. *Theor. Found. Chem. Eng.* **2007**, *41*(4), 451-453.

(14) Lang, P.; Yatim, H.; Moszkowicz, P.; Otterbein, M. Batch Extractive Distillation under Constant Reflux Ratio. *Comput. Chem. Eng.* **1994***, 18*, 1057-1069.

(15) Lang, P., Lelkes, Z., Moszkowicz P., Otterbein M., Yatim H., Different operational policies for the batch extractive distillation, *Comp. Chem. Eng.* **1995**, *19*, S645.

(16) Gmehling, J.; Onken, U. *Vapour – Liquid Equilibrium Data Collection. DECHEMA Chemistry Data Series.* Vol. 1. (12 parts); Frankfurt am Main. **1982**.

(17) Frits, E.R; Lelkes, Z.; Fonyo, Z.; Rev, E.; Markot, M.Cs. Finding Limiting Flows of Batch Extractive Distillation with Interval Arithmetics. AIChE J. 2006, 52(9), 3100-3108.

(18) Knapp, J. P.; Doherty, M. F. Minimum Entrainer Flow for Extractive Distillation: A Bifurcation Theoretic Approach. AIChE J. 1994, 40(2), 243-268.

FIGURE CAPTION

Figure 1. Ternary diagram for the separation of low α binary mixtures by using homogeneous heavy entrainers with no forming additional azeotropes
Figure 2. Influence of the reflux and the entrainer feed flowrate on extractive singular points of the class 0.0-1 diagrams. No univolatility lines exist.
Figure 3. Reflux and entrainer feed flowrate influence on the extractive singular points of class 0.0-1 diagram involving the univolatility line α_{AB}.
Figure 4. Heptane – toluene – phenol thermodynamic properties and composition profiles for $F_E/V = 0.5$ (a) infinite reflux (b) $R = 5$.
Figure 5. Heptane – toluene – chlorobenzene thermodynamic properties and liquid composition profiles for $F_E/V = 0.5$ (a) infinite reflux (b) $R = 5$.
Figure 6. Residue curve map, univolatility line α_{AB}, volatility order and extractive stable node range for the ethyl acetate – benzene - n-hexanol mixture.
Figure 7. Ethyl acetate – benzene – n-hexanol rectifying and extractive liquid composition profiles for $F_E/V = 0.1$ (a) infinite reflux (b) $R = 50$.
Figure 8. Simulation results for the separation of the mixture ethyl acetate – benzene using n-hexanol by extractive batch distillation for F_E/V=0.1 and R=50.
Figure 9. Extractive composition profile map and simulation results for the separation of the mixture ethyl acetate – benzene with n-hexanol at F_E/V=0.5 and infinite reflux.
Figure 10. Map of extractive and rectifying composition profile for F_E/V=0.5 and R=20. (a) ethyl acetate and (b) benzene as first distillate cut.

Figure 11. Simulation results for the separation of the mixture ethyl acetate – benzene with n-hexanol at F_E/V=0.5 and R=20 for the initial still compositions x_{S1} and x_{S2}.

Figure 12. Extractive composition profiles map and simulations results considering F_E/V=2 and infinite R. Separation of ethyl acetate – benzene using n-hexanol.
Figure 13. Rectifying and extractive composition profile map for the separation for the mixture ethyl acetate – benzene – n hexanol at F_E/V=2 and R=50.

Figure 14. Simulations results for the separation of ethyl acetate – benzene using n-hexanol considering the initial still composition x_{S10} into the feasible region (I) and x_{S20} into the unfeasible region (II).

Figure 15. Residue curve map for the ternary mixture ethyl acetate – benzene – n butanol.
Figure 16. Extractive composition profile map of the mixture ethyl acetate – benzene – 1-butanol for F_E/V=0.1 and F_E/V=1 at infinite reflux ratio.
Figure 17. Extractive composition profile map of the mixture ethyl acetate – benzene – 1 butanol for F_E/V=1 and R=50.
Figure 18. Simulation results of the separation of the mixture ethyl acetate – benzene using 1 butanol for F_E/V=2 and R=30.

Class 0.0-1

(a) *diagram 1 / occurrence : 71.6%*

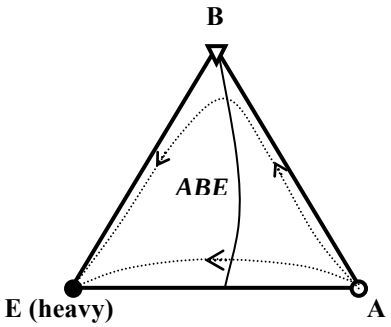

(b) *diagram 2 / occurrence : 11.3%*

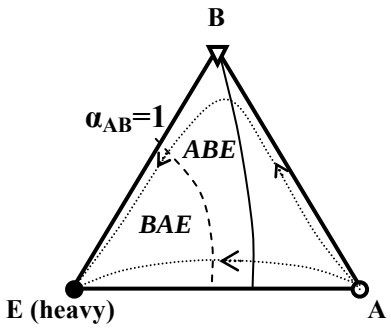

(c) *diagram 3 / occurrence : 11.0%*

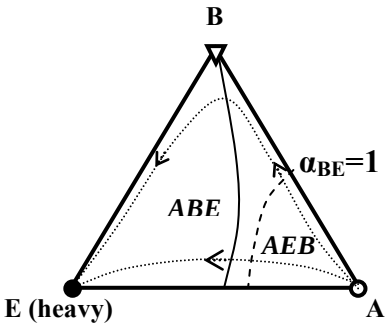

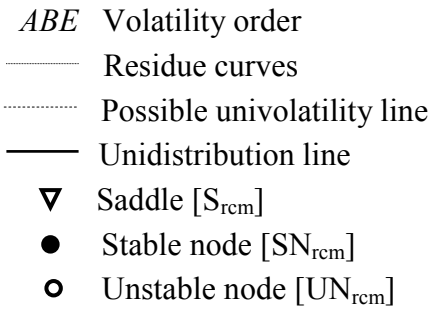

Figure 1. Ternary diagram for the separation of low α binary mixtures by using homogeneous heavy entrainers with no forming additional azeotropes

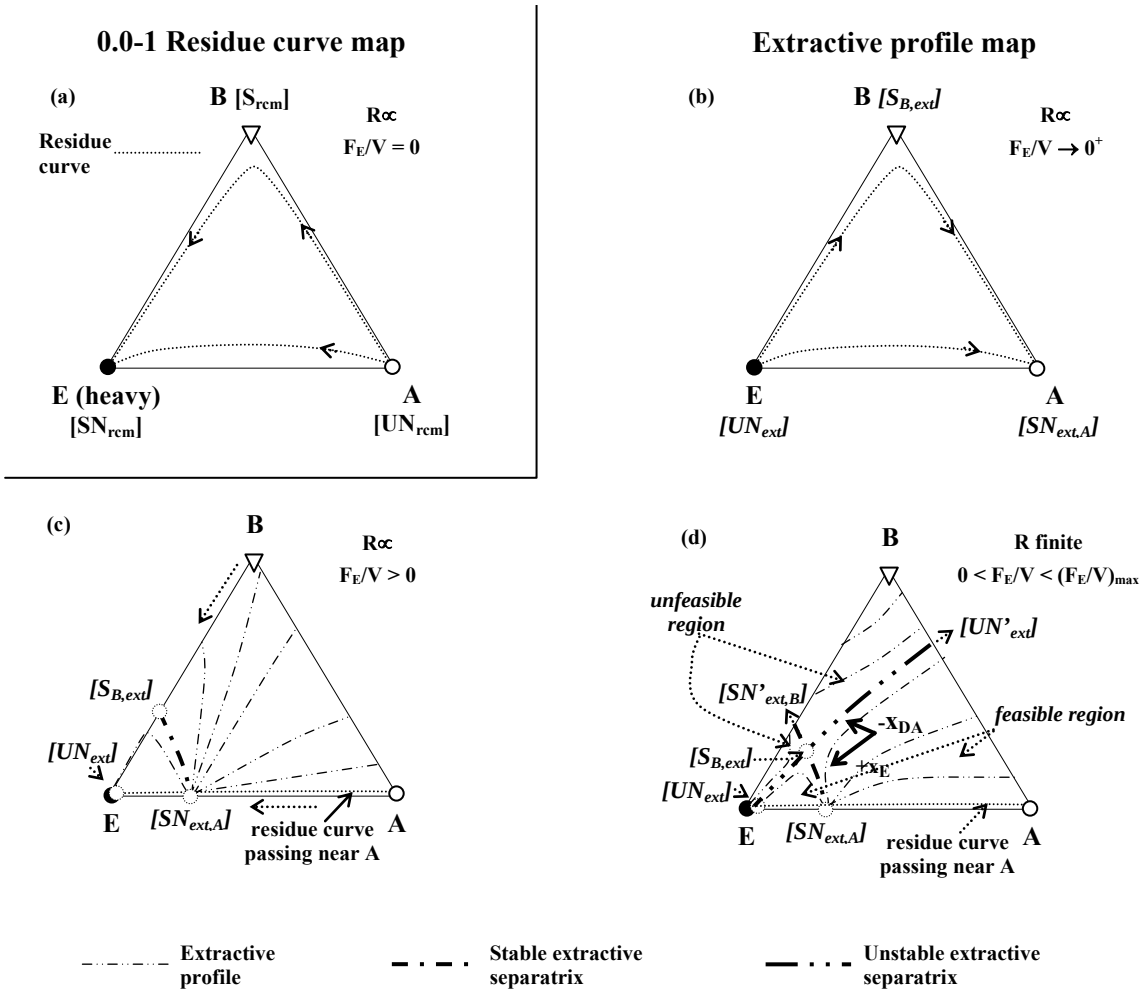

Figure 2. Influence of the reflux and the entrainer feed flowrate on extractive singular points of the class 0.0-1 diagrams. No univolatility lines exist.

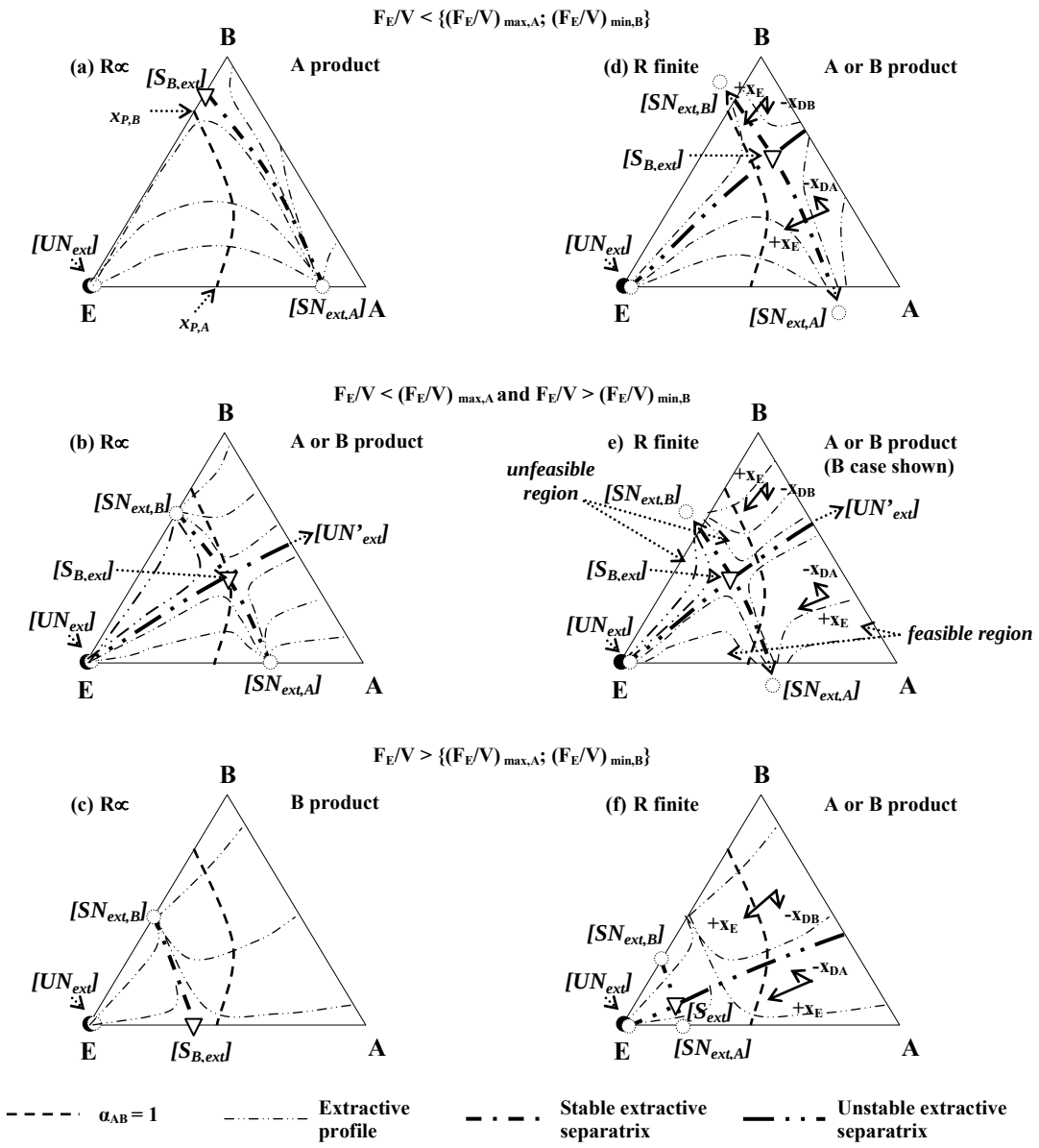

Figure 3. Reflux and entrainer feed flowrate influence on the extractive singular points of class 0.0-1 diagram involving the univolatility line α_{AB}.

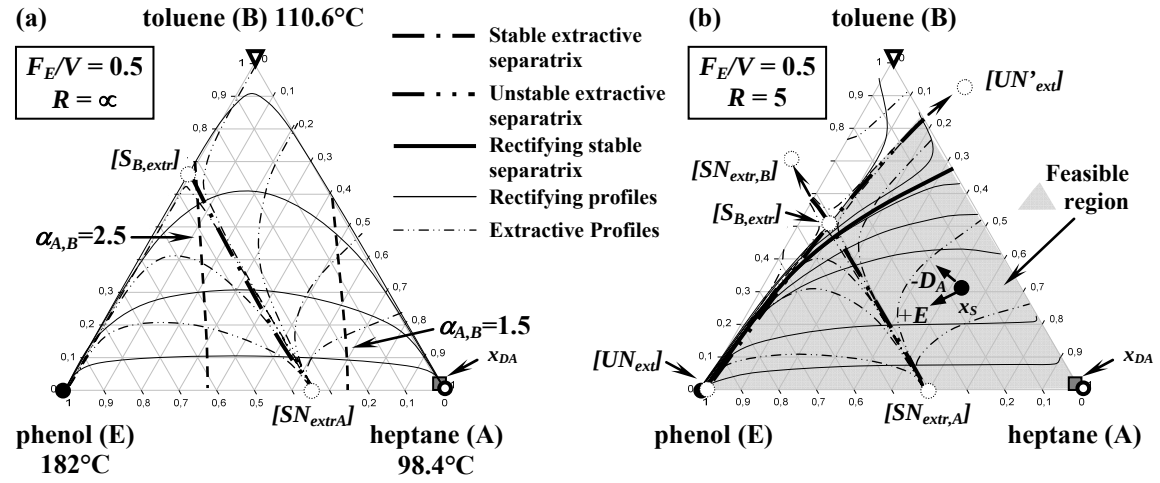

Figure 4. Heptane – toluene – phenol thermodynamic properties and composition profiles for $F_E/V = 0.5$ (a) infinite reflux (b) $R = 5$.

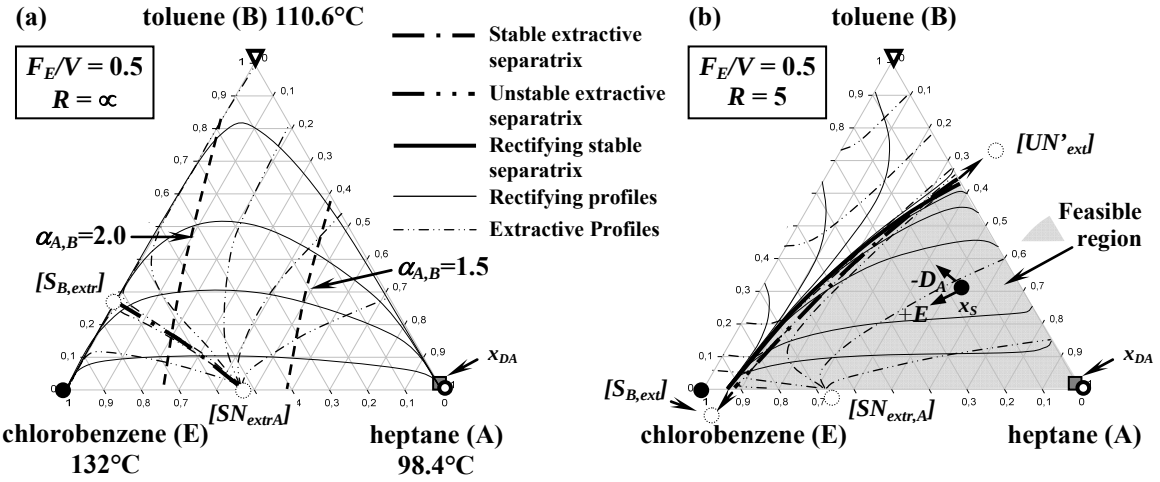

Figure 5. Heptane – toluene – chlorobenzene thermodynamic properties and liquid composition profiles for $F_E/V = 0.5$ (a) infinite reflux (b) $R = 5$.

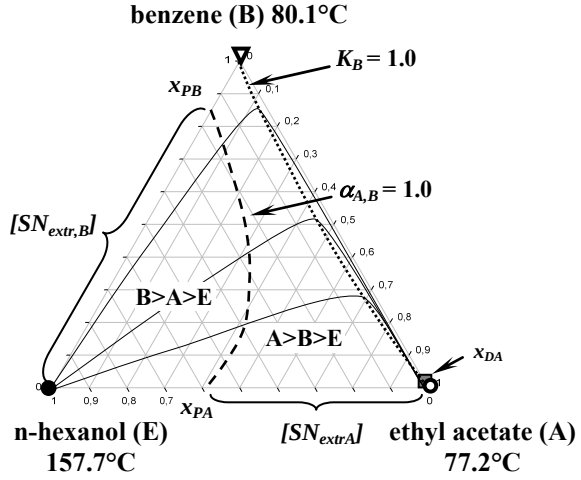

Figure 6. Residue curve map, univolatility line α_{AB}, volatility order and extractive stable node range for the ethyl acetate – benzene - n-hexanol mixture.

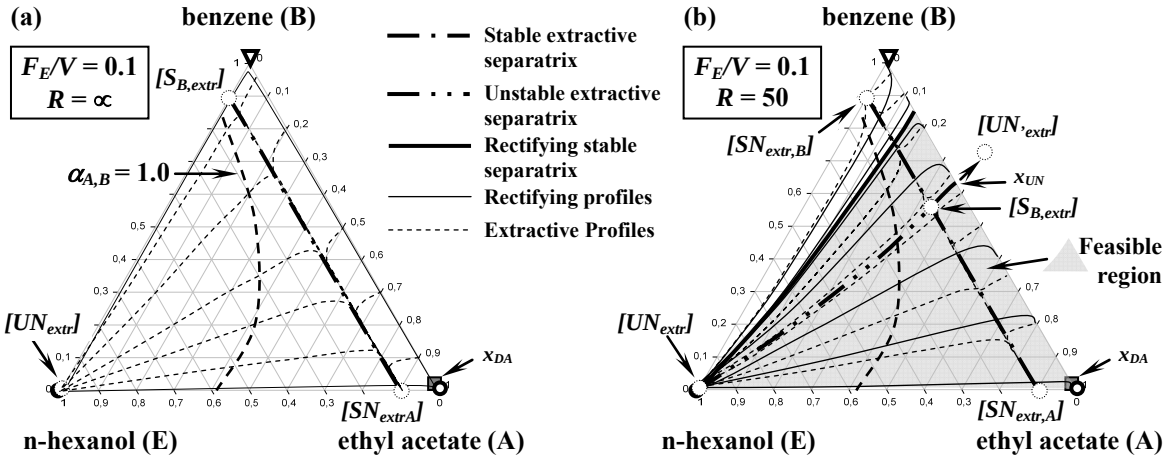

Figure 7. Ethyl acetate – benzene – n-hexanol rectifying and extractive liquid composition profiles for $F_E/V = 0.1$ (a) infinite reflux (b) $R = 50$.

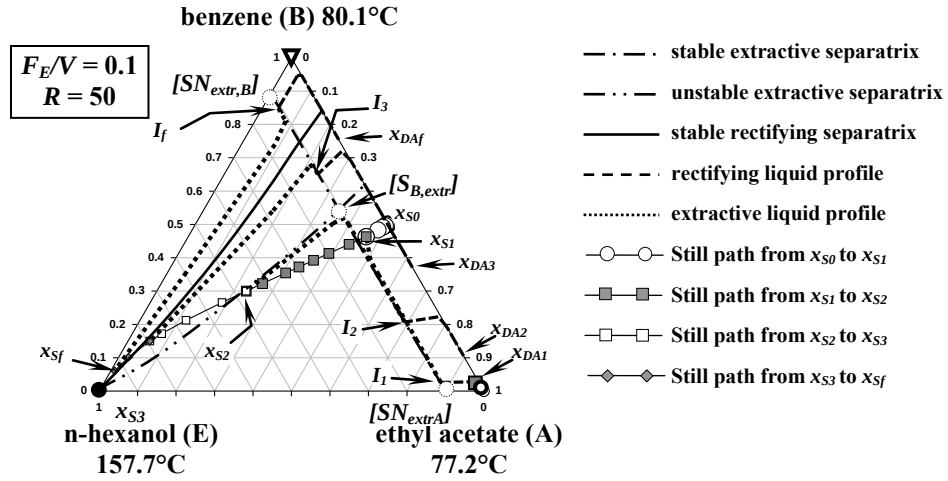

Figure 8. Simulation results for the separation of the mixture ethyl acetate – benzene using n-hexanol by extractive batch distillation for F_E/V=0.1 and R=50.

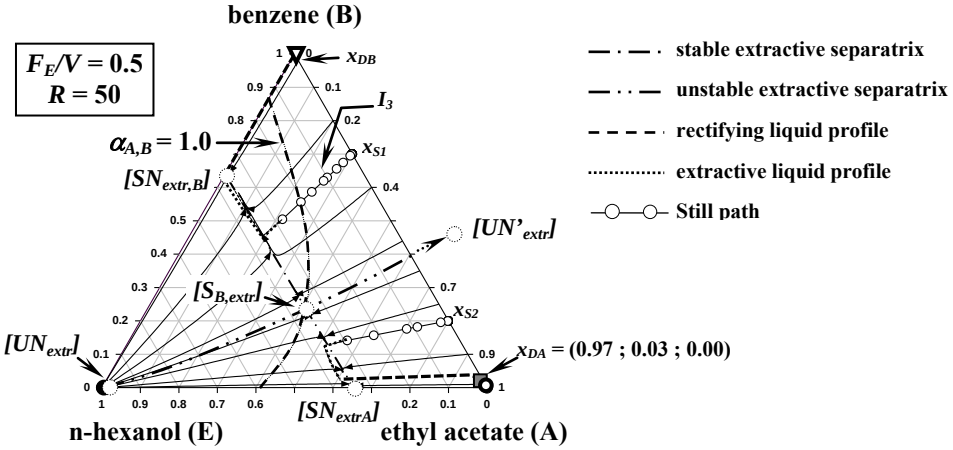

Figure 9. Extractive composition profile map and simulation results for the separation of the mixture ethyl acetate – benzene with n-hexanol at F_E/V=0.5 and infinite reflux.

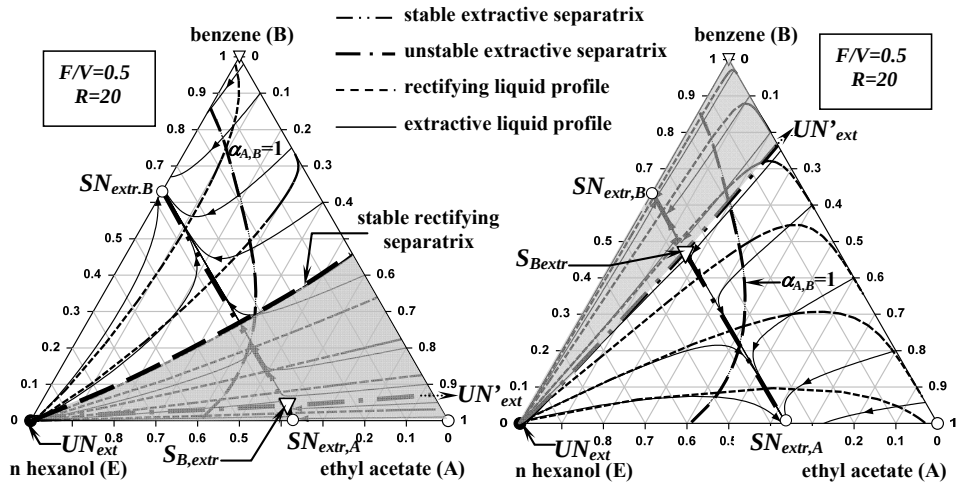

(a) x_{DA}=(0.98, 0.01, 0.01) **(b)** x_{DB}=(0.01, 0.98, 0.01)

Figure 10. Map of extractive and rectifying composition profile for F_E/V=0.5 and R=20. (a) ethyl acetate and (b) benzene as first distillate cut.

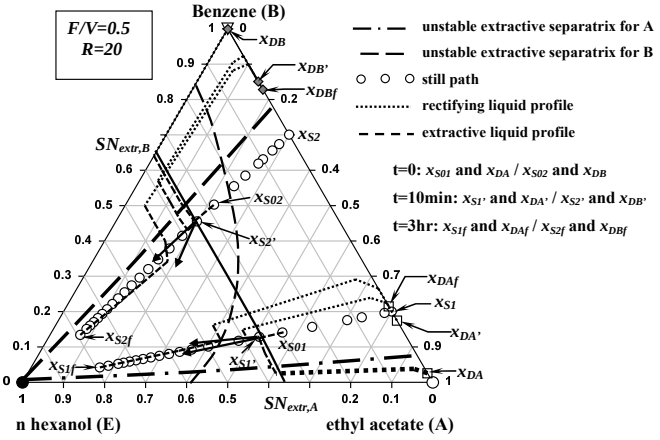

Figure 11. Simulation results for the separation of the mixture ethyl acetate – benzene with n-hexanol at F_E/V=0.5 and R=20 for the initial still compositions x_{S1} and x_{S2}.

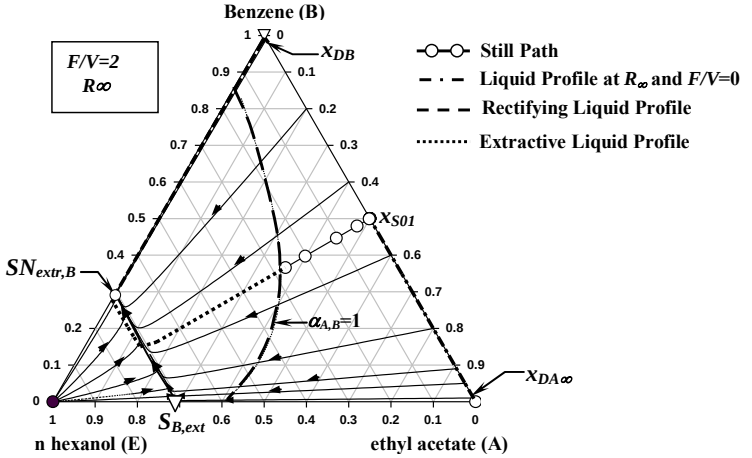

Figure 12. Extractive composition profiles map and simulations results considering F_E/V=2 and infinite R. Separation of ethyl acetate – benzene using n-hexanol.

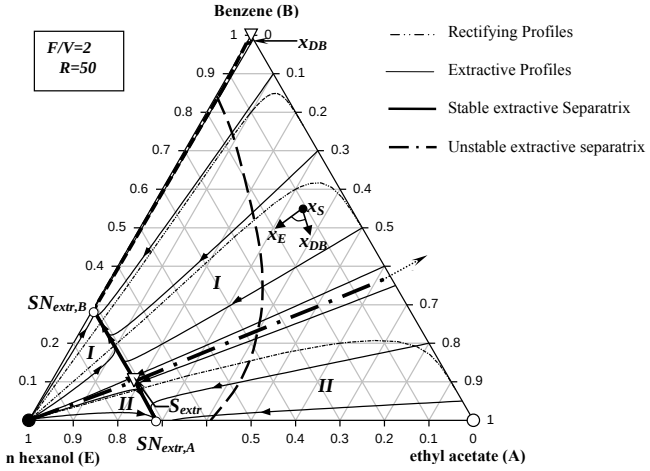

Figure 13. Rectifying and extractive composition profile map for the separation for the mixture ethyl acetate – benzene – n hexanol at F_E/V=2 and R=50.

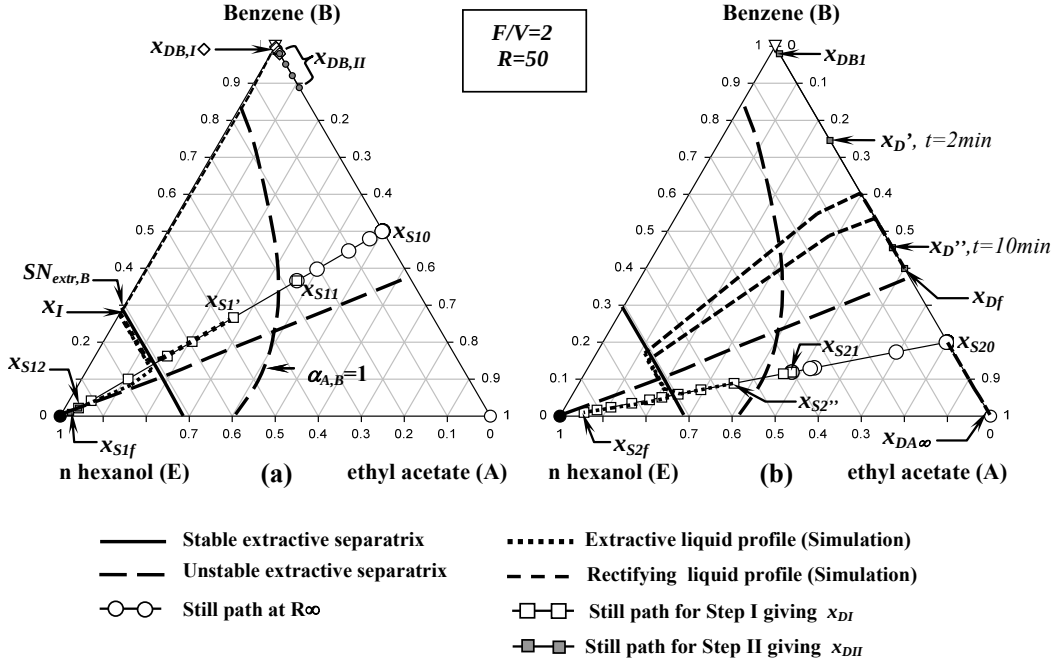

Figure 14. Simulations results for the separation of ethyl acetate – benzene using n-hexanol considering the initial still composition x_{S10} into the feasible region (I) and x_{S20} into the unfeasible region (II).

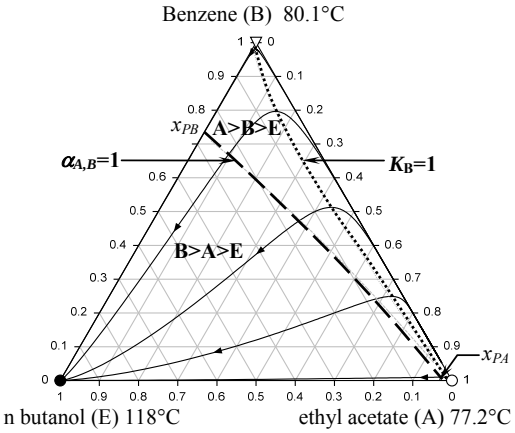

Figure 15. Residue curve map for the ternary mixture ethyl acetate – benzene – n butanol.

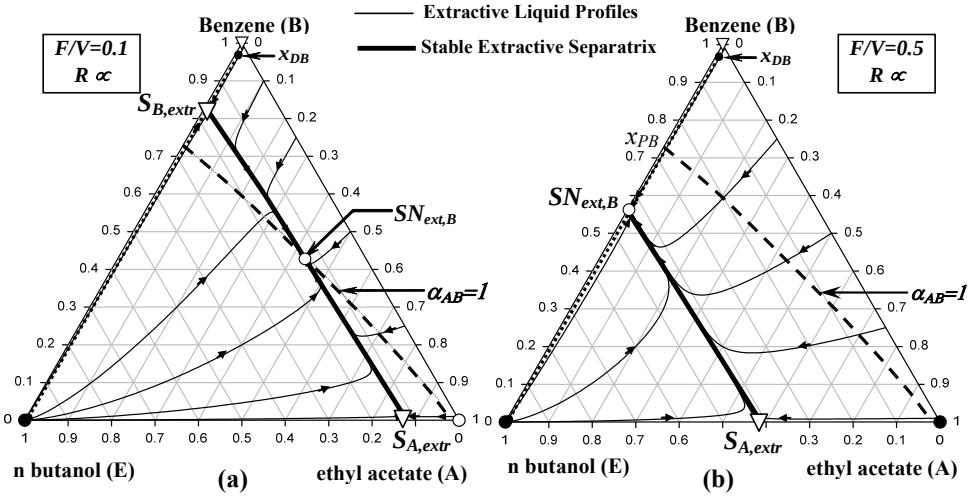

Figure 16. Extractive composition profile map of the mixture ethyl acetate – benzene – 1-butanol for F_E/V=0.1 and F_E/V=1 at infinite reflux ratio.

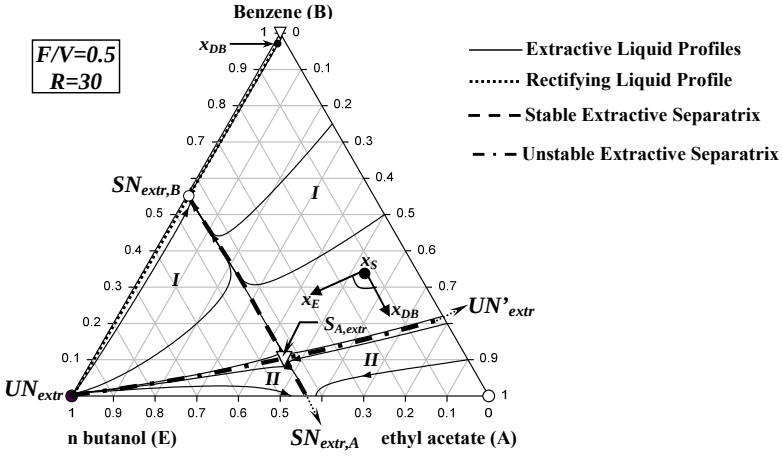

Figure 17. Extractive composition profile map of the mixture ethyl acetate – benzene – 1 butanol for F_E/V=1 and R=50.

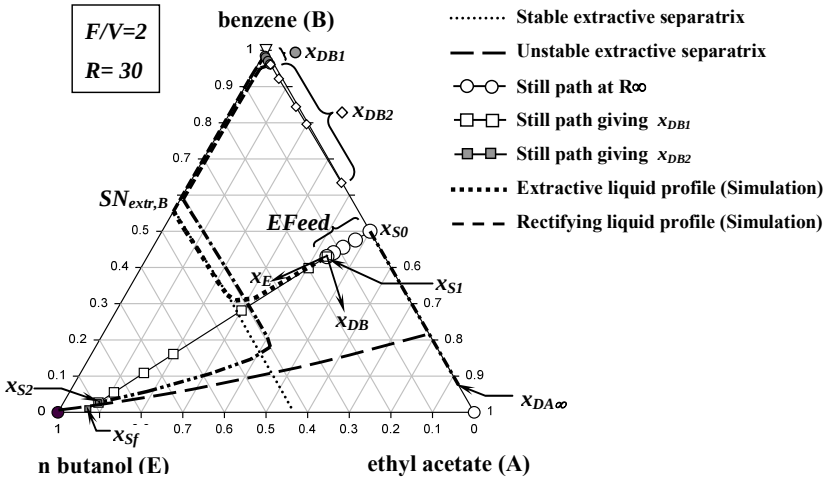

Figure 18. Simulation results of the separation of the mixture ethyl acetate – benzene using 1 butanol for F_E/V=2 and R=30.

TABLE CAPTION

Table 1. Binary coefficients for computing the ternary liquid – vapour equilibrium.[16]

Table 2. Binary coefficients for computing the ternary liquid – vapour equilibrium.[16]

Binary Coefficients [cal/mol]	Model	A_{ij}	A_{ji}	α_{ij}
Heptane (A) – toluene (B)		-30.576	268.334	0.2986
Heptane (A) – phenol (E)	NRTL	1120.08	701.706	0.2930
Toluene (B) – phenol (E)		847.767	-64.343	0.2994
Heptane (A) – toluene (B)		-30.576	268.334	0.2986
Heptane (A) – chlorobenzene (E)	NRTL*	-66.7486	552.464	0.2994
Toluene (B) – chlorobenzene (E)		-403.054	479.892	0.3042
Ethyl acetate (A) – Benzene (B)				
Ethyl acetate (A) – n hexanol (E)	UNIFAC			
Benzene (B) – n hexanol (E)				
Ethyl acetate (A) – Benzene (B)		204.816	-202.045	-
Ethyl acetate (A) – n butanol (E)	UNIQUAC	568.262	-321.007	-
Benzene (B) – n butanol (E)		390.866	-100.608	-

* Varga (2006)